

**DUFOUR, RADIATION AND HALL EFFECTS ON UNSTEADY MHD FLOW
OF VISCOUS INCOMPRESSIBLE FLUID PAST AN INCLINED PLATE EMBEDDED
IN POROUS MEDIUM WITH THERMAL STRATIFICATION**

N. PANDYA*, MOHAMMAD SULEMAN QURAISHI**

***Department of Mathematics & Astronomy,
University of Lucknow - 226007, Lucknow, India.**

****Department of Mathematics & Astronomy,
University of Lucknow - 226007, Lucknow, India.**

(Received On: 06-10-17; Revised & Accepted On: 08-11-17)

ABSTRACT

In this research article it is investigated that Dufour, Hall and radiation effects on unsteady MHD flow of a viscous incompressible fluid past an inclined porous plate immersed in porous medium with Thermal stratification. The governing equations of non-dimensional forms of flow field have been solved numerically using Crank-Nicolson implicit finite difference method. The results are obtained for velocities, temperature and concentration. The effects of various parameters are discussed on flow variables and are presented through graphs and tables.

Keywords: MHD, Dufour effect, Hall effect, Thermal radiation, Thermal Stratification, porous medium, heat and mass transfer, Crank-Nicolson finite difference method.

INTRODUCTION

In engineering and applied physics, Dufour, Hall and radiation effects play important role. The analysis of such flow has been applied in MHD generators, chemical engineering, geothermal energy and astrophysical study. The existence of pure fluid in nature is rather impossible. Molecules are transported in multi component mixture driven by temperature gradient, is known as Soret effect and inverse phenomena is Dufour effect. Hall effect arises in plasma when electrons are able to drift with magnetic field but ions cannot. Sparrow and Cess [1] investigated the effect of magnetic field on free convection heat transfer. Jana and Kanch [2] have analyzed hall effect on unsteady Couette flow under boundary layer approximation. Rao *et al.* [3] studied chemical reaction effects on an unsteady MHD free convective flow past an infinite vertical porous plate with constant suction and heat source. Ghosh [4] has investigated the effects of hall current on MHD Couette flow in a rotating system with arbitrary magnetic field. Nadeem *et al.* [5] studied the effects of Hall current on unsteady flow of a Non-Newtonian fluid in a rotating system. Pandya and Shukla [6] investigated Soret Dufour and radiation effects on unsteady MHD flow past an impulsively started inclined porous plate with variable temperature and mass diffusion. Laxmi *et al.* [7] analyzed numerically the effects of Dufour and Soret on an unsteady MHD flow past an infinite vertical porous plate with thermal radiation. Ram Reddy [8] studied effects of Soret and Dufour on mixed convection heat and mass transfer in a micro polar fluid with heat and mass flows. Bhaben N Ch. Neog, Rudra KT. Deka [9] discussed Combined Effect of **Thermal Stratification** and Radiation on Unsteady Natural Convection MHD Flow Past an Impulsively Started Infinite Vertical Plate in Fluid Saturated Porous medium. N. Pandya, A.K. Shukla [10] investigated Soret-Dufour, radiation and Hall effects on unsteady MHD flow of a viscous incompressible fluid past an inclined plate imbedded in porous medium.

The objective of this paper is to analyze the effects of Dufour, Hall and radiation on inclined porous plate in presence of variable temperature and concentration with thermal stratification. The governing equation of non-dimensional form of flow fields are solved numerically using Crank-Nicolson implicit finite difference method. The effect of difference physical parameters on velocity, temperature and concentration are discussed through graphically.

Corresponding Author: Mohammad Suleman Quraishi**

****Department of Mathematics & Astronomy, University of Lucknow-226007, Lucknow, India.**

MATHEMATICAL FORMULATION OF THE PROBLEM

Consider an unsteady MHD flow of a viscous incompressible electrically conducting fluid past an infinite inclined porous plate with variable temperature and concentration and Dufour, radiation and Hall effects with thermal stratification has been studied. The plate is embedded in porous medium and inclined at angle λ to vertical. x' -axis is taken along the plate and y' -axis is normal to it. A uniform magnetic field B_0 is taken in y' -axis and plate is electrically non-conducting. Consider z' -axis normal to xy plane.

Let velocity \vec{V}' and magnetic field \vec{H}' have components (u', v', w') and (H_x', H_y', H_z') respectively.

Equation of continuity:

$$\frac{\partial v'}{\partial y'} = 0, \Rightarrow v' = -v_0 \text{ (constant)} \quad (1)$$

From Maxwell's electromagnetic field equations, $\frac{\partial H_y'}{\partial y'} = 0$ (2)

Here magnetic Reynolds number is very- very small, so induced magnetic field is negligible in comparison to applied magnetic field, hence

$$H_x' = 0 = H_z' \text{ and } H_y' = B_0 \quad (3)$$

Let (J_x', J_y', J_z') be components of electric current density \vec{J}' , by conservation of electric charge $\nabla \cdot \vec{J}' = 0$ implies $J_y' = \text{constant}$ (4)

On Account of non conducting plate $J_y' = 0$. To neglect polarized effect,

We have $\vec{E}' = 0$ (5)

Hence $\vec{J}' = (J_x', 0, J_z')$, $\vec{H}' = (0, B_0, 0)$ and $\vec{V}' = (u', v_0, w')$ (6)

Taking Hall effect into account, the generalized Ohm's law

$$\vec{J}' + \frac{\omega_e \tau_e}{B_0} (\vec{J}' \times \vec{H}') = \sigma \left(\vec{E}' + \vec{V}' \times \vec{H}' + \frac{1}{en_e} \nabla p_e \right) \quad (7)$$

Where \vec{V}' , ω_e , τ_e , e , η_e , p_e , σ , \vec{E}' are velocity vector, electron frequency, electron collision time, electron charge, number of density of electron, electron pressure, electric conductivity and electric field respectively. It is considered that $\omega_e \tau_e \approx 0$

From equation (6) and (7), we have

$$\vec{J}'_x = \frac{\sigma B_0}{1+m^2} (mu' - w') \text{ and } \vec{J}'_z = \frac{\sigma B_0}{1+m^2} (u' + mw') \quad (8)$$

Here u' along x' -axis and w' along z' -axis and $m = \omega_e \tau_e$ is Hall parameter.

Momentum equations

$$\frac{\partial u'}{\partial t'} = \nu \frac{\partial^2 u'}{\partial y'^2} + g \beta \cos \lambda (T' - T_\infty') + g \beta^* \cos \lambda (C' - C_\infty') - \frac{\sigma B_0^2}{\rho(1+m^2)} (u' + mw') - \frac{\nu u'}{K'} \quad (9)$$

$$\frac{\partial w'}{\partial t'} = \nu \frac{\partial^2 w'}{\partial y'^2} + \frac{\sigma B_0^2}{\rho(1+m^2)} (mu' - w') - \frac{\nu w'}{K'} \quad (10)$$

Energy equation

$$\frac{\partial T'}{\partial t'} = \frac{k}{\rho C_p} \frac{\partial^2 T'}{\partial y'^2} - \frac{\partial q_r}{\partial y'} \frac{1}{\rho C_p} + \frac{D_m K_T}{C_p C_s} \frac{\partial^2 C'}{\partial y'^2} - \gamma u' \quad (11)$$

Equation of mass transfer

$$\frac{\partial C'}{\partial t'} = D \frac{\partial^2 C'}{\partial y'^2} - K_r (C' - C'_\infty) \quad (12)$$

Here $\gamma = \frac{dT'_\infty}{dy'} + \frac{g}{C_p}$ is thermal stratification parameter. The environment is statically stable, neutral or unstable

according as $\gamma >, =$ or < 0 . Here, $\frac{dT'_\infty}{dy'}$ is the thermal stratification term and $\frac{g}{C_p}$ is the pressure work term known as compression. Inclusion of $\gamma u'$ term in the energy equation makes the flow situation more realistic in nature because the two equations become coupled. As a result both the temperature and the velocity fields are interdependent.

Here molecular diffusivity is D_m , coefficient of volume expansion for mass transfer is β^* , volumetric coefficient of thermal expansion is β , magnetic induction is B_0 , velocity component along x -axis, y' -axis and z -axis are u' , v' and w' respectively, permeability of porous medium is K' , electrical conductivity is σ , gravitational acceleration is g , fluid density is ρ , thermal conductivity of fluid is k , specific heat of constant pressure is C_p , thermal diffusion ratio is K_T , dimensional temperature is T' temperature of free stream is T'_∞ , dimensional concentration is C' , concentration of free stream is C'_∞ , kinematic viscosity is ν , radiation of heat flux along y' -axis is q_r , mean fluid temperature is T_m .

Boundary and initial conditions are given as:

$$\begin{aligned} t' \leq 0; \quad u' = 0, \quad w' = 0, \quad T' = T'_\infty, \quad C' = C'_\infty \quad \forall y' \\ t' > 0; \quad u' = u_0, \quad v' = -v_0, \quad w' = 0, \quad T' = T' + (T'_w - T'_\infty) e^{At'} \\ C' = C' + (C'_w - C'_\infty) e^{At'} \quad \text{at } y' = 0 \\ u' = 0, \quad w' = 0, \quad T' \rightarrow T'_\infty, \quad C' \rightarrow C'_\infty \quad y' \rightarrow \infty \end{aligned} \quad (13)$$

Where $A = \frac{\gamma u_0}{\Delta T'}$, temperature and concentration of plate are T'_w and C'_w respectively. To use the Roseland approximation, radiative heat flux is given by

$$q_r = -\frac{4\sigma}{3k_m} \frac{\partial T'^4}{\partial y'} \quad (14)$$

Here Stefan Boltzmann constant and absorption coefficient are σ and k_m respectively. In this case temperature difference are very-very small withinflow, such that T'^4 can be expressed linearly with temperature. It is realized by expanding in a Taylor series about T'_∞ and neglecting higher order terms, so

$$T'^4 \cong 4T'^3_\infty T' - 3T'^4_\infty \quad (15)$$

Hence, by equation 14 and equation 15, equation 11 is reduced as

$$\frac{\partial T'}{\partial t'} = \frac{k}{\rho C_p} \frac{\partial^2 T'}{\partial y'^2} + \frac{16\sigma T'^3_\infty}{3k_m} \frac{\partial^2 T'}{\partial y'^2} \frac{1}{\rho C_p} + \frac{D_m K_T}{C_p C_s} \frac{\partial^2 C'}{\partial y'^2} - \gamma u' \quad (16)$$

In order to produce non-dimensional partial differential equations, introducing following dimensional less quantities:

$$\begin{aligned} t = \frac{t' \gamma u_0}{\Delta T'}, \quad y = y' \sqrt{\frac{\gamma u_0}{\nu \Delta T'}}, \quad \theta = \frac{T' - T'_\infty}{T'_w - T'_\infty}, \quad u = \frac{u'}{u_0}, \quad C = \frac{C' - C'_\infty}{C'_w - C'_\infty}, \quad K = \frac{\gamma u_0 K'}{\nu \Delta T'}, \quad A = \frac{\gamma u_0}{\Delta T'}, \\ M = \frac{\sigma B_0^2 \Delta T'}{\gamma \rho u_0}, \quad P_r = \frac{\nu \rho C_p}{k}, \quad R = \frac{4\sigma T'^3_\infty}{k_m k P_r}, \quad S_c = \frac{\nu}{D}, \quad K_r = \frac{k_r (T'_w - T'_\infty)}{\gamma u_0}, \\ Du = \frac{D_m K_T (C' - C'_\infty)}{C_s C_p \nu (T'_w - T'_\infty)}, \quad \Delta T' = T'_w - T'_\infty, \quad w = \frac{w'}{w_0} \\ G_r = \frac{g \beta (T'_w - T'_\infty)^2}{\gamma u_0^2}, \quad G_m = \frac{g \beta (C'_w - C'_\infty) \Delta T'}{\gamma u_0^2} \end{aligned} \quad (17)$$

In view of equations 17, we yield dimensionless form of equations 9, 10, 12 and 16 respectively

$$\frac{\partial u}{\partial t} = \frac{\partial^2 u}{\partial y^2} + G_r \theta \cos \lambda + G_m C \cos \lambda - \left(\frac{M}{1+m^2} + \frac{1}{K} \right) u - \left(\frac{mM}{1+m^2} \right) w \quad (18)$$

$$\frac{\partial w}{\partial t} = \frac{\partial^2 w}{\partial y^2} - \left(\frac{M}{1+m^2} + \frac{1}{K} \right) w + \left(\frac{mM}{1+m^2} \right) u \quad (19)$$

$$\frac{\partial \theta}{\partial t} = -u + \frac{1}{P_r} \left(1 + \frac{4R}{3} \right) \frac{\partial^2 \theta}{\partial y^2} + D_u \frac{\partial^2 C}{\partial y^2} \quad (20)$$

$$\frac{\partial C}{\partial t} = \frac{1}{S_c} \frac{\partial^2 C}{\partial y^2} - K_r C \quad (21)$$

With boundary conditions:

$$\begin{aligned} t \leq 0; \quad u = 0, \quad w = 0, \quad \theta = 0, \quad C = 0 \quad \forall y \\ t > 0; \quad u = 1, \quad w = 0, \quad \theta = e^t, \quad C = e^t \quad \text{at } y = 0 \\ u \rightarrow 0, \quad w \rightarrow 0, \quad \theta \rightarrow 0, \quad C \rightarrow 0 \quad y \rightarrow \infty \end{aligned} \quad (22)$$

Now, it is useful to calculate physical quantities for primary interest, these are coefficient of skin-friction at the wall along x-axis τ_1 , coefficient of skin-friction at the wall along z-axis τ_2 , Nusselt number Nu and Sherwood number Sh . Dimensionless forms of these physical quantities are:

$$\tau_1 = \left(\frac{\partial u}{\partial y} \right)_{y=0}, \tau_2 = \left(\frac{\partial w}{\partial y} \right)_{y=0}, Nu = - \left(\frac{\partial \theta}{\partial y} \right)_{y=0}, Sh = - \left(\frac{\partial C}{\partial y} \right)_{y=0} \quad (23)$$

Method of Solution:

Equations 18 to 21 are linear partial differential equations, are solved using initial boundary conditions 22, it is solved by Crank-Nicolson implicit finite difference method for numerical solution. Equations 18, 19, 20 and 21 are expressed as:

$$\begin{aligned} \frac{u_{i,j+1} - u_{i,j}}{\Delta t} = & \left(\frac{u_{i-1,j} - 2u_{i,j} + u_{i+1,j} + u_{i-1,j+1} - 2u_{i,j+1} + u_{i+1,j+1}}{2(\Delta y)^2} \right) \\ & + G_r \cos \lambda \left(\frac{\theta_{i,j+1} + \theta_{i,j}}{2} \right) + G_m \cos \lambda \left(\frac{C_{i,j+1} + C_{i,j}}{2} \right) - \left(\frac{M}{1+m^2} + \frac{1}{K} \right) \left(\frac{u_{i,j+1} + u_{i,j}}{2} \right) \\ & - \left(\frac{mM}{1+m^2} \right) \left(\frac{w_{i,j+1} + w_{i,j}}{2} \right) \end{aligned} \quad (24)$$

$$\begin{aligned} \frac{w_{i,j+1} - w_{i,j}}{\Delta t} = & \left(\frac{w_{i-1,j} - 2w_{i,j} + w_{i+1,j} + w_{i-1,j+1} - 2w_{i,j+1} + w_{i+1,j+1}}{2(\Delta y)^2} \right) \\ & - \left(\frac{M}{1+m^2} + \frac{1}{K} \right) \left(\frac{w_{i,j+1} + w_{i,j}}{2} \right) + \left(\frac{mM}{1+m^2} \right) \left(\frac{u_{i,j+1} + u_{i,j}}{2} \right) \end{aligned} \quad (25)$$

$$\begin{aligned} \frac{\theta_{i,j+1} - \theta_{i,j}}{\Delta t} = & - \left(\frac{u_{i,j+1} + u_{i,j}}{2} \right) \\ & + \frac{1}{P_r} \left(1 + \frac{4R}{3} \right) \left(\frac{\theta_{i-1,j} - 2\theta_{i,j} + \theta_{i+1,j} + \theta_{i-1,j+1} - 2\theta_{i,j+1} + \theta_{i+1,j+1}}{2(\Delta y)^2} \right) \\ & + D_u \left(\frac{C_{i-1,j} - 2C_{i,j} + C_{i+1,j} + C_{i-1,j+1} - 2C_{i,j+1} + C_{i+1,j+1}}{2(\Delta y)^2} \right) \end{aligned} \quad (26)$$

$$\begin{aligned} \frac{C_{i,j+1} - C_{i,j}}{\Delta t} = & \frac{1}{S_c} \left(\frac{C_{i-1,j} - 2C_{i,j} + C_{i+1,j} + C_{i-1,j+1} - 2C_{i,j+1} + C_{i+1,j+1}}{2(\Delta y)^2} \right) \\ & - K_r \left(\frac{C_{i,j+1} + C_{i,j}}{2} \right) \end{aligned} \quad (27)$$

Corresponding boundary and initial conditions are

$$\begin{aligned} u_{i,0} &= 0, & w_{i,0} &= 0, & \theta_{i,0} &= 0, & C_{i,0} &= 0 \quad \forall i \\ u_{0,j} &= 1, & w_{0,j} &= 0, & \theta_{0,j} &= e^{j^* \Delta t}, & C_{0,j} &= e^{j^* \Delta t} \\ u_{L,j} &\rightarrow 0, & w_{L,j} &\rightarrow 0, & \theta_{L,j} &\rightarrow 0, & C_{L,j} &\rightarrow 0 \end{aligned} \quad (28)$$

Here, index I refers to y and j to time, $\Delta t = t_{j+1} - t_j$ and $\Delta y = y_{i+1} - y_i$. For known values of u, w, Theta and C at t, we calculate these values for t + Δt as follows, after substitution of i=1, 2, 3... L-1, where L corresponds to ∞ . Now equations 24 to 27 systems of equations is solved by Thomas Algorithm as discussed in Carnahan *et al.* [9]. Then θ and C are known for all values of y at t + Δt . Replacing values of θ and C in equations 24, 25 and solved by same with initial and boundary conditions, we have solutions for u and w till desired time t. Crank-Nicolson implicit finite difference method is second order method ($O(\Delta t^2)$) in time and has no limitation for space and time steps, that is, the method is unconditionally stable. Computation has been executed for $\Delta y=0.1$, $\Delta t=0.001$ and repeated till $y=4$.

RESULT AND DISCUSSION

With reference of physical problem, numerical results for dimensionless velocities u and w, temperature θ and concentration C are discussed with help of graphs by assigning numerical values of thermal Grashof number Gr, solute Grashof number Gm, Dufour number Du, Schmidt number Sc, Prandtl number Pr, radiation parameter R, Hall parameter m, magnetic parameter M, permeability of porous medium K, Chemical reaction parameter Kr and inclination angle λ .

Fig.1, 2, 3, 4, 6, 8 and 11 depicts that the primary velocity 'u' increases with increase in Gr, Gm, K, t, R, m and Du.

Fig. 5, 7, 9, 10 and 12 show that velocity 'u' decreases with increase in Sc, P_r , M, Kr and λ .

Fig.13 and 15 for Secondary velocity 'w' described that 'w' decreases with increase in t and P_r .

Fig. 14, 17 and 18 shows that 'w' increases with increase in R, M and K respectively.

A Special effect of hall parameter is observed in Fig.16 that 'w' increases first with two increasing values of m and then 'w' decreases with two other increasing values of m.

Temperature profile θ , in Fig. 19, 20 and 22, shows increase with increment in t, R and Du parameters respectively and decreases with increment in P_r in Fig. 21.

Concentration profile 'C' increases with time 't' in Fig. 25 and decreases with increment in K_r and S_c in Fig. 23 and 24 respectively.

Table 1 depict that on increasing λ , S_c , M and K_r skin friction coefficient τ_1 along wall x-axis decreases and increases with increment in Du , K , R and M while skin friction coefficient τ_2 along wall z-axis decreases as λ , S_c and K_r increase and τ_2 increases on increasing Du , K and R . Table 1 displays also that τ_2 increases first and then decreases with increment in M and m . It is also analyzed in Table1 that Nusselt number Nu increases on increasing K and m , decreases on increasing S_c , Du , K_r , R , M and λ on the other hand Sherwood number increases with increase in K_r and S_c while Sh is approximately equal when increment in Du , K , R , M , m and λ .

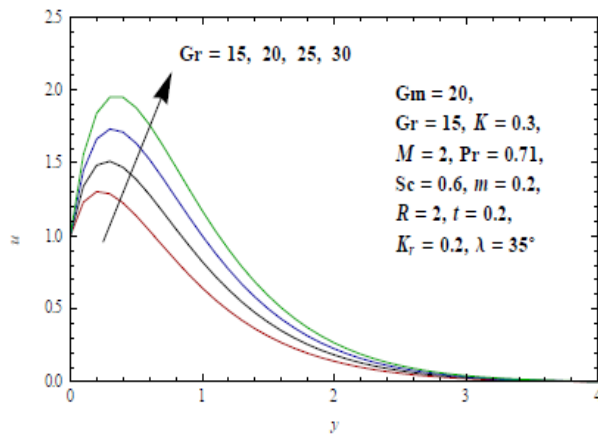


Figure-1: Velocity profile u for different values of Gr

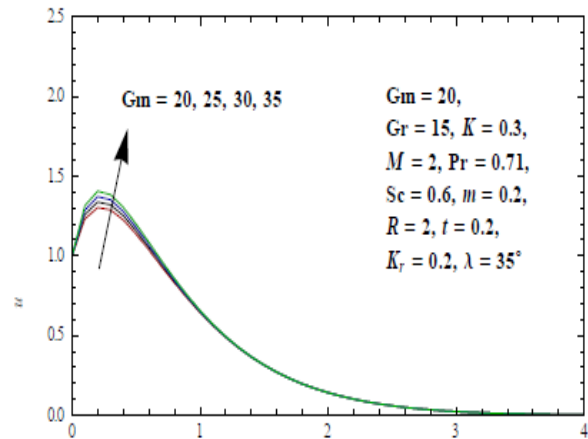


Figure-2: Velocity profile u for different values of Gm

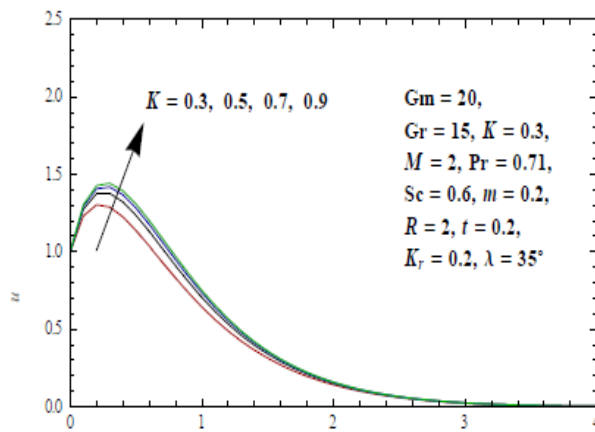


Figure-3: Velocity profile u for different values of K

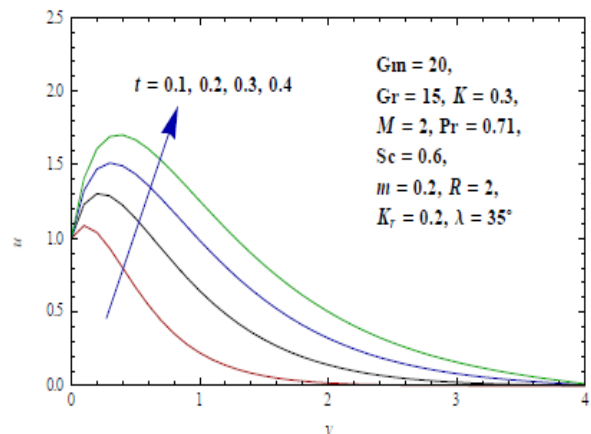


Figure-4: Velocity profile u for different values of t

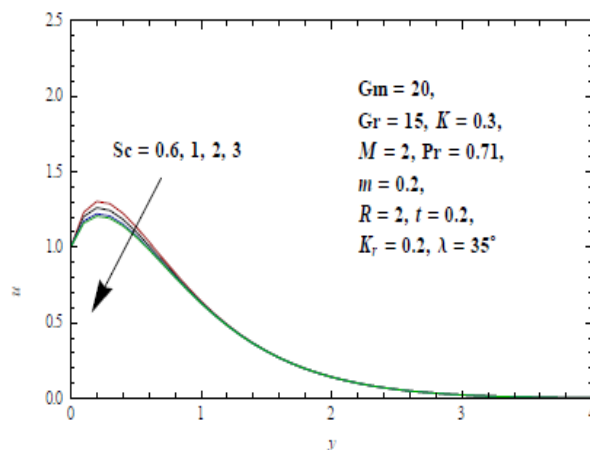


Figure-5: Velocity profile u for different values of Sc

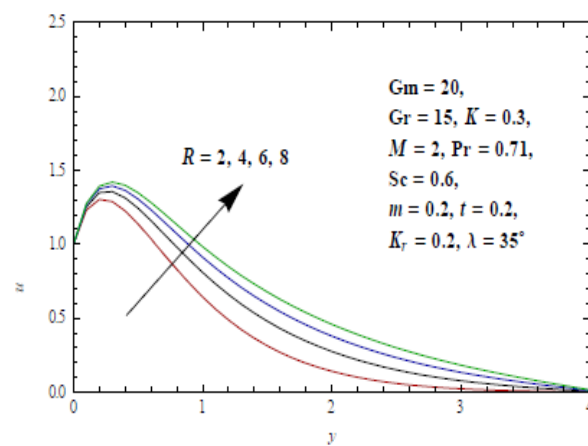


Figure-6: Velocity profile u for different values of R

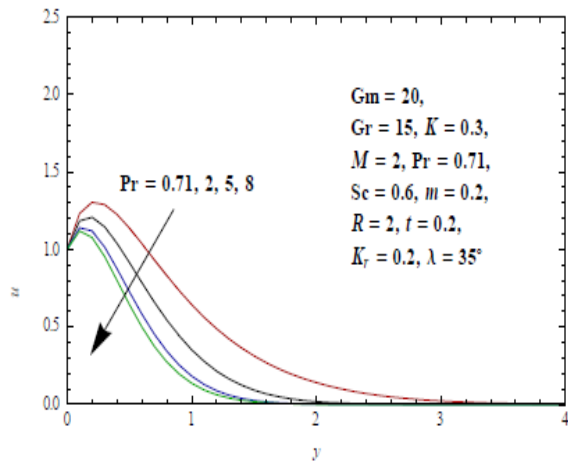


Figure-7: Velocity profile u for different values of Pr

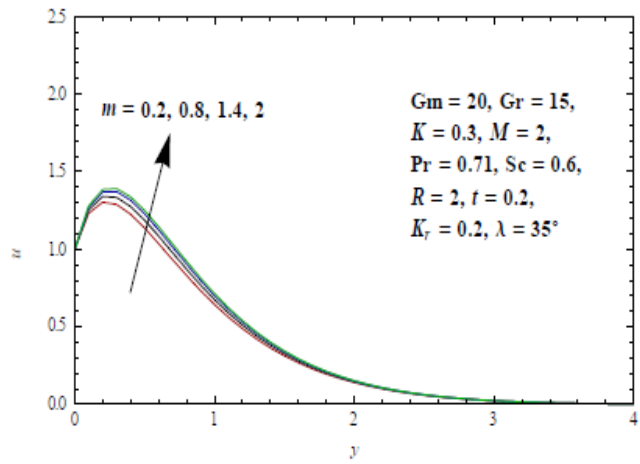


Figure-8: Velocity profile u for different values of m

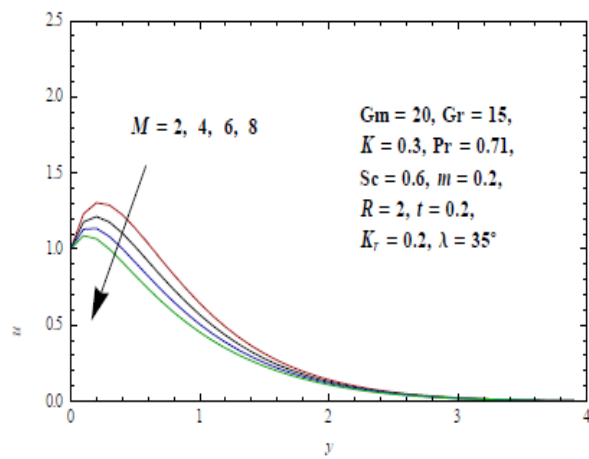


Figure-9: Velocity profile u for different values of M

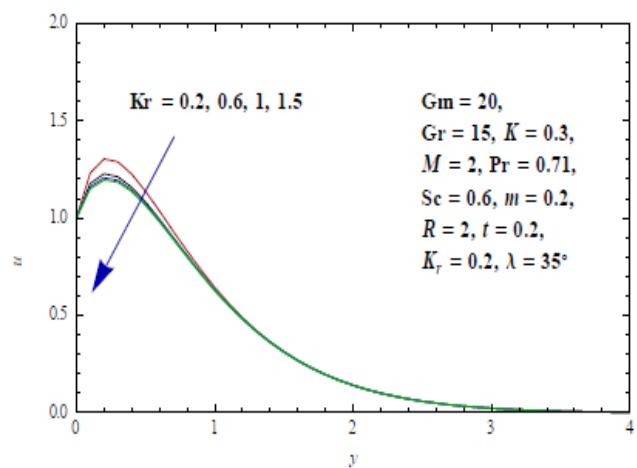


Figure-10: Velocity profile u for different values of K_r

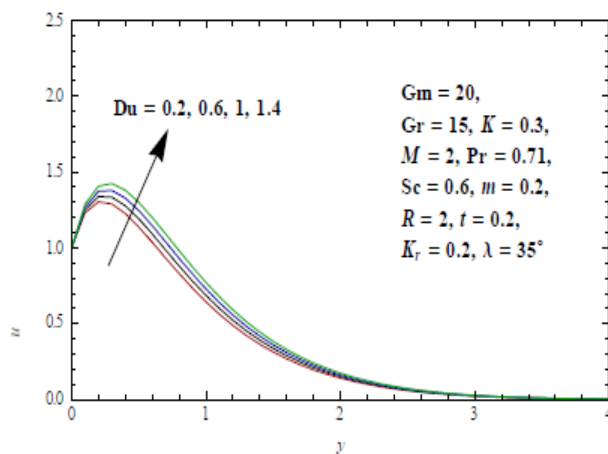


Figure-11: Velocity profile u for different values of D_u

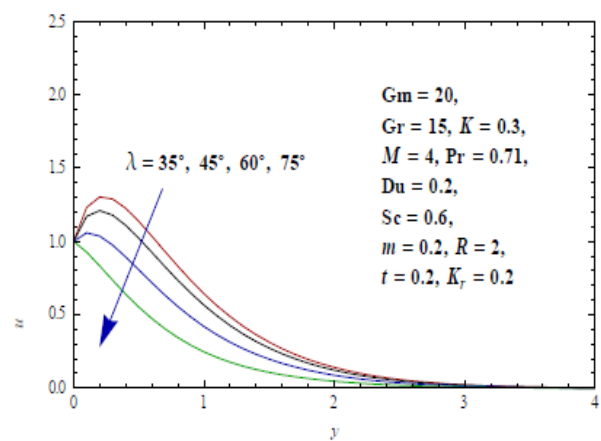


Figure-12: Velocity profile u for different values of λ

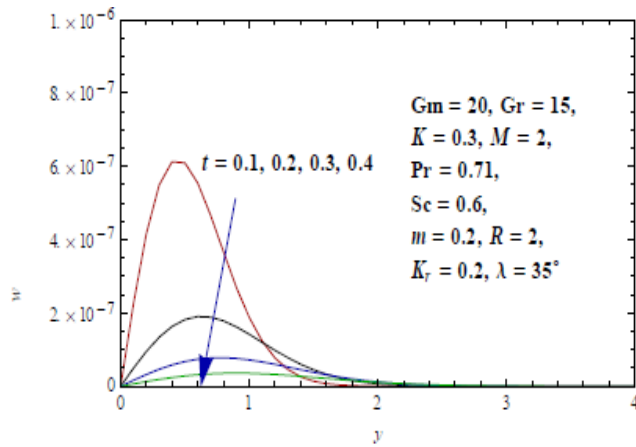


Figure-13: Velocity profile w for different values of t

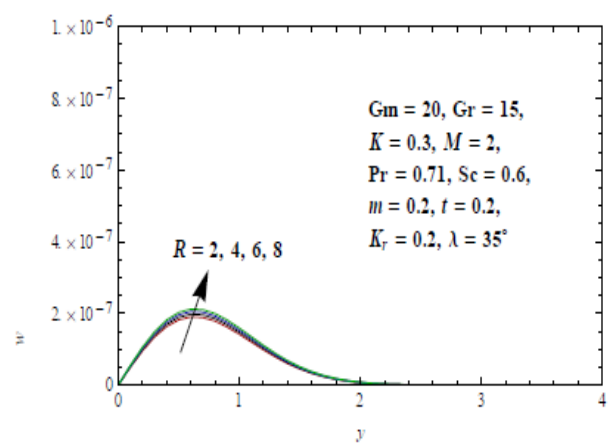


Figure-14: Velocity profile w for different values of R

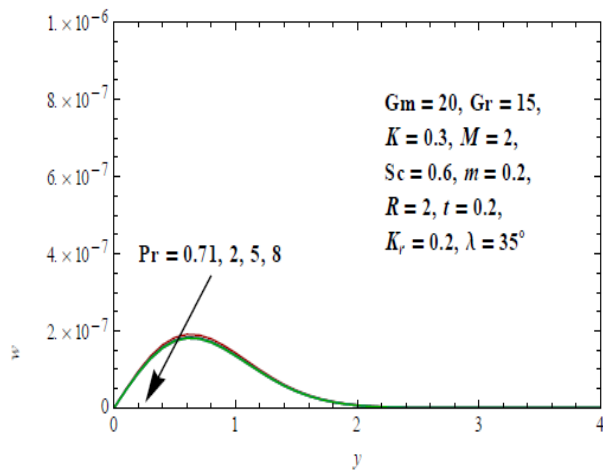


Figure-15: Velocity profile w for different values of Pr

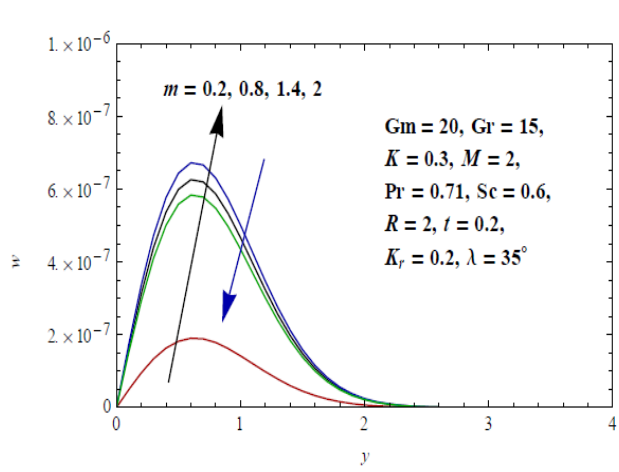


Figure-16: Velocity profile w for different values of m

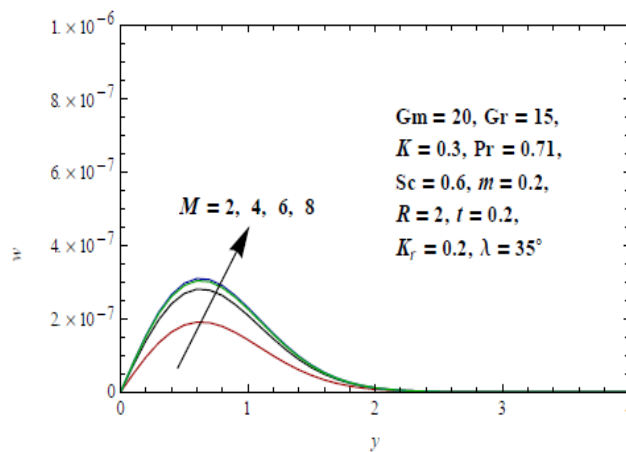


Figure-17: Velocity profile w for different values of M

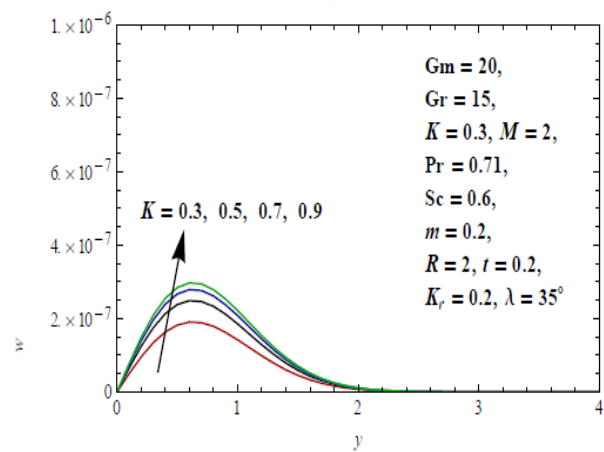


Figure-18: Velocity profile w for different values of K

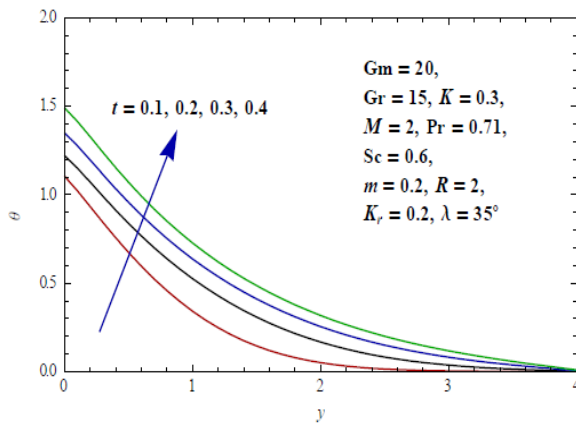


Figure-19: Temperature profile for different values of t

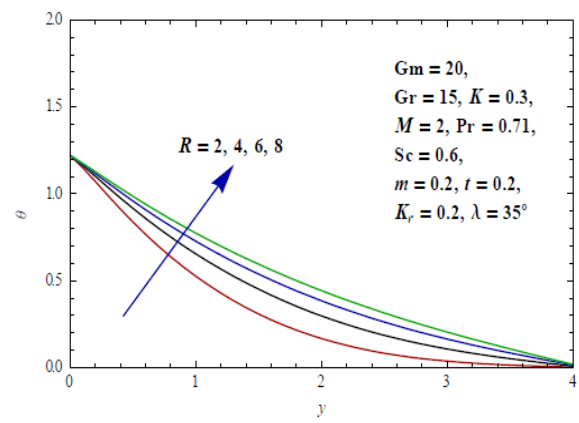


Figure-20: Temperature profile for different values of R

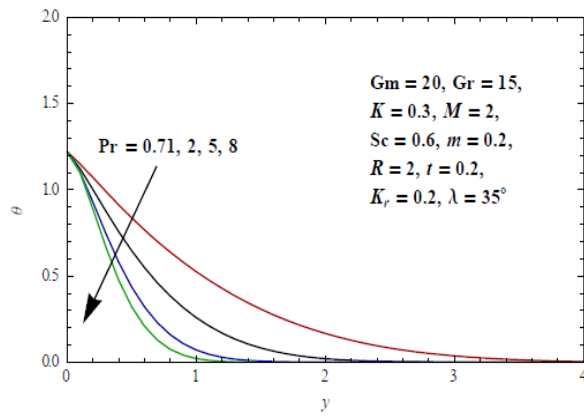


Figure-21: Temperature profile for different values of Pr

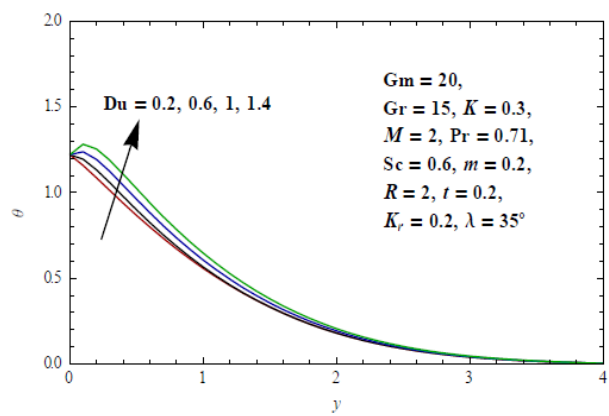


Figure-22: Temperature profile for different values of Du

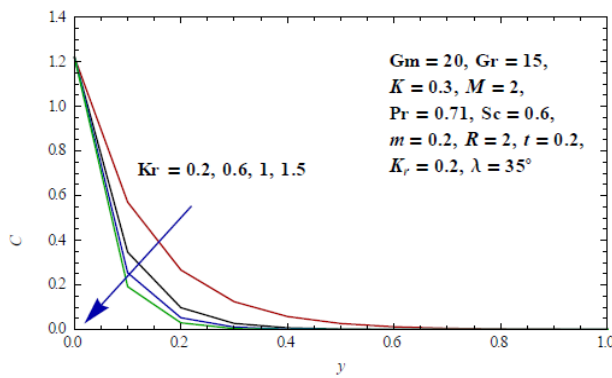


Figure-23: Concentration profile for different values of Kr

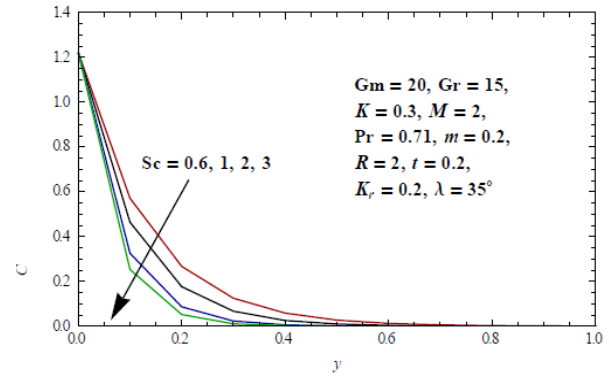


Figure-24: Concentration profile for different values of Sc

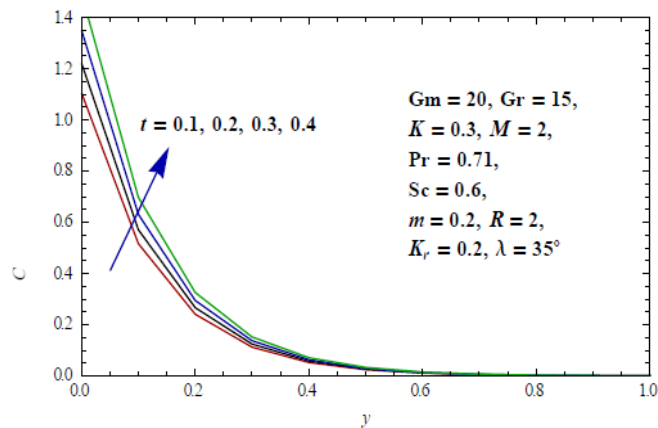


Figure-25: Concentration profile for different values of t

Table-1: Skin friction coefficient τ_1 and τ_2 for different values of parameters

D _u	K	Kr	Sc	R	M	m	λ	τ_1	τ_2	Nu	Sh
0.2	0.3	0.2	0.6	2	2	0.2	35	2.31498	4.93586*10 ⁻⁷	0.705537	6.50213
0.6	0.3	0.2	0.6	2	2	0.2	35	2.5058	4.95715*10 ⁻⁷	0.266998	6.50213
1	0.3	0.2	0.6	2	2	0.2	35	2.69663	4.97845*10 ⁻⁷	-0.171541	6.50213
1.4	0.3	0.2	0.6	2	2	0.2	35	2.88745	4.99974*10 ⁻⁷	-0.610079	6.50213
0.2	0.5	0.2	0.6	2	2	0.2	35	2.73565	6.44372*10 ⁻⁷	0.713482	6.50213
0.2	0.7	0.2	0.6	2	2	0.2	35	2.92915	7.22359*10 ⁻⁷	0.717161	6.50213
0.2	0.9	0.2	0.6	2	2	0.2	35	3.04037	7.69694*10 ⁻⁷	0.719282	6.50213
0.2	0.3	0.6	0.6	2	2	0.2	35	1.77281	4.91887*10 ⁻⁷	0.613069	8.74618
0.2	0.3	1	0.6	2	2	0.2	35	1.60163	4.90638*10 ⁻⁷	0.576023	9.66814
0.2	0.3	1.5	0.6	2	2	0.2	35	1.49874	4.89475*10 ⁻⁷	0.551224	10.2901
0.2	0.3	0.2	1	2	2	0.2	35	2.03042	4.89158*10 ⁻⁷	0.660984	7.56944
0.2	0.3	0.2	2	2	2	0.2	35	1.73032	4.85811*10 ⁻⁷	0.604391	8.96007
0.2	0.3	0.2	3	2	2	0.2	35	1.59888	4.8469*10 ⁻⁷	0.575456	9.68139
0.2	0.3	0.2	0.6	4	2	0.2	35	2.54189	5.12586*10 ⁻⁷	0.5751	6.50213
0.2	0.3	0.2	0.6	6	2	0.2	35	2.67297	5.3071*10 ⁻⁷	0.500643	6.50213
0.2	0.3	0.2	0.6	8	2	0.2	35	2.76112	5.48048*10 ⁻⁷	0.452517	6.50213
0.2	0.3	0.2	0.6	2	4	0.2	35	1.77459	7.25994*10 ⁻⁷	0.695461	6.50213
0.2	0.3	0.2	0.6	2	6	0.2	35	1.29963	8.01057*10 ⁻⁷	0.686756	6.50213
0.2	0.3	0.2	0.6	2	8	0.2	35	0.878568	7.85849*10 ⁻⁷	0.679185	6.50213
0.2	0.3	0.2	0.6	2	2	0.8	35	2.53181	1.62208*10 ⁻⁶	0.709623	6.50213
0.2	0.3	0.2	0.6	2	2	1.4	35	2.70727	1.74293*10 ⁻⁶	0.712944	6.50213
0.2	0.3	0.2	0.6	2	2	2	35	2.79897	1.51271*10 ⁻⁶	0.714685	6.50213
0.2	0.3	0.2	0.6	2	2	0.2	45	1.70984	4.88113*10 ⁻⁷	0.694341	6.50213
0.2	0.3	0.2	0.6	2	2	0.2	60	0.586773	4.77997*10 ⁻⁷	0.673517	6.50213
0.2	0.3	0.2	0.6	2	2	0.2	75	-0.728525	4.66217*10 ⁻⁷	0.649056	6.50213

CONCLUSIONS

In this work we have concluded that Dufour, Hall and radiation effects on unsteady MHD flow of a viscous incompressible fluid past an inclined porous plate immersed in porous medium with Thermal stratification concluded the following conclusions:

1. Increasing inclination angle and Prandlt number, Primary velocity 'u' decreases rapidly.
2. Increasing Thermal Grashof number and time, Primary velocity 'u' increases rapidly.
3. Primary velocity 'u' slowly increases with Dufour, Magnetic and Hall parameters.
4. Secondary velocity 'w' rapidly increases with Magnetic parameter, and with hall parameter and then decreases.
5. Secondary velocity 'w' rapidly decreases with time.
6. Temperature increases with time and decreases Prandlt number.
7. Concentration increases with t.
8. Concentration decreases with increase in Schmidt number and chemical reaction parameter.

REFERENCES

1. Sparrow,E.M. and Cess,R.D ,(1961), Effect of Magnetic Field on Free Convection Heat Transfer, Int. J. Heat Mass Transfer, 3, pp. 267-270.
2. Jana,R.N. and Kanch,A.K., (2001), Hall effect on Unsteady Couette Flow Boundary Layer Approximation, J. Phys. Scie., 7, pp. 74-86.
3. Rao,j.A. and Shivaiah,S., (2011), Chemical Reaction on an Unsteady MHD free Convective Flow past and Infinite Vertical Porous Plate with Constant Suction and Heat Source, Int. J. of Appl. Math. and Mech., 7(8), pp. 98-118.
4. Ghosh,S.K., (2002), Effect of Hall Current on MHD Couette Flow in a Rotating System with arbitrary Magnetic Field, Czech. J. Phys., 52(1), pp. 51-63.
5. Hayat,J., Nadeem,S., Asghar,S. and Siddiqui,A.M., (2005), Effect of Hall Current on Unsteady Flow of a second grade Fluid in Rotating System, Chem. Eng. Comm., 192, pp. 1272-1284.
6. Pandya,N. and Shukla,A.K., (2013), Soret Dufour and Radiation effects on Unsteady MHD flow past an impulsively started inclined Porous Plate with variable temperature and mass diffusion, Int. J. Math. And Sci. Comp., 3(2), pp. 41-48.

7. Vempati,S.R. and Laxmi Narayan Gari,A.B., (2010), Soret and Dufour Effects on Unsteady MHD flow past an infinite vertical porous plate with Thermal radiation, App. Math. Mech. Eng. Ed., 31(12), pp. 1481-1496.
8. SrinivaSacharya,D. and Ram Reddy,Ch., (2010), Effects of Soret and Dufour on mixed Convection Heat and Mass Transfer in a Micro Polar Fluid with Heat and Mass fluxes, Int. J. of Appl. Math. and Mech., 6(21).
9. Bhaben N Ch. Neog, Rudra KT. Deka , Combined Effect of Thermal Stratification and Radiation on Unsteady Natural Convection MHD Flow Past an Impulsively Started Infinite Vertical Plate in Fluid Saturated Porous medium, Proceedings of the 6th WSEAS International Conference on HEAT and MASS TRANSFER (HMT'09)
10. N. Pandya, A.K. Shukla, Soret-Dufour, Radiation and Hall effects on unsteady MHD flow of a viscous incompressible fluid past an inclined plate embedded in porous medium, TWMS Journal of Applied and Engineering Mathematics Vol.6, No.1, © I, sik University, Department of Mathematics, 2016, pp. 163-174.

Source of support: Nil, Conflict of interest: None Declared.

[Copy right © 2017. This is an Open Access article distributed under the terms of the International Journal of Mathematical Archive (IJMA), which permits unrestricted use, distribution, and reproduction in any medium, provided the original work is properly cited.]